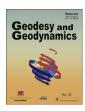


Contents lists available at ScienceDirect

# Geodesy and Geodynamics

journal homepages: www.keaipublishing.com/en/journals/geog; http://www.jgg09.com/jweb\_ddcl\_en/EN/volumn/home.shtml



# Global spectral model of the geoid



The Key Laboratory of Geospace Environment and Geodesy, School of Geodesy and Geomatics, Wuhan University, 430079, China



#### ARTICLE INFO

Article history:
Received 13 October 2016
Accepted 7 December 2016
Available online 22 December 2016

Keywords: Density Earth Gravity Topography

#### ABSTRACT

The coefficients of the Global Gravitational Models (GGMs) define the external gravitational field of the Earth. In many geoscience applications and gravity interpretations these coefficients are routinely used to represent the geoid surface and related gravitational field quantities without taking into consideration the internal convergence domain for computing the gravitational field inside the Earth's masses. In this study we discuss this issue and present the numerical approach for computing the gravitational field quantities on the geoid. The proposed numerical approach utilizes spectral expressions for the gravimetric forward modelling of topographic mass density distribution and the indirect gravimetric modelling of mass density heterogeneities inside the geoid. In the numerical realization we demonstrate that for precise applications the differences between the potential values computed at the topographic surface and on the geoid should be taken into consideration especially in mountainous regions with complex geology as well as in polar regions, where these differences in absolute values reach 40 m<sup>2</sup> s<sup>-2</sup> (or more), which translates into vertical displacements between the geoid and the quasigeoid of about 4 m.

© 2016 Institute of Seismology, China Earthquake Administration, etc. Production and hosting by Elsevier B.V. on behalf of KeAi Communications Co., Ltd. This is an open access article under the CC BY-NC-ND license (http://creativecommons.org/licenses/by-nc-nd/4.0/).

### 1. Introduction

The gravity-dedicated satellite missions, Challenging Minisatellite Payload (CHAMP) [1], the Gravity Recovery and Climate Experiment (GRACE) [2] and the Gravity Field and Steady-State Ocean Circulation Explorer (GOCE) [3] significantly improved our knowledge on the external gravitational field of the Earth at the long-to-medium wavelengths (approximately up to the spherical harmonic degree of 250–280). The CHAMP, GRACE and GOCE data have been facilitated in various geoscience studies. In climate studies, for instance, the geoid is used as a reference surface for a definition of the mean dynamic topography (i.e., the vertical displacement of the mean sea surface from the geoid) for interpreting the global oceanic circulation including its temporal variations (e.g., [4,5]) and other climatic phenomena. In geophysics, the

E-mail address: rtenzer@sgg.whu.edu.cn.

Peer review under responsibility of Institute of Seismology, China Earthquake Administration.



Production and Hosting by Elsevier on behalf of KeAi

long-to-medium spectrum of the gravitational field has been used to investigate mantle convection, tectonics, sub-lithospheric stress and isostatic mechanisms. This is possible, because the long-wavelength gravitational spectrum comprise mainly the signature of deep mantle density heterogeneities while the medium-to-short wavelengths are dominated by the signal from more shallow sources within the lithosphere including the terrain geometry (on land) and the ocean-floor relief (offshore). For more details we refer readers to studies, for instance, by [6–22]. Moreover, these global gravitational models were also used to recover the Moho interface (e.g., [23,24]).

The external gravitational field of the Earth (as observed by the gravity-dedicated satellite missions) can directly be used to model the geoid and related gravitational field quantities over the world's oceans and marginal seas. Over continents, however, the geoid determination from the external gravitational field model requires applying the topographic correction (cf. [25]). In global studies this factor is often ignored, assuming that the gravitational contribution of topography (including the terrain and topographic density variations) propagates mainly to a short-wavelength (higher-degree) spectrum of the gravitational field while its long-wavelength effect is small or completely negligible.

In this study we demonstrate that this assumption is not supported by numerical results. Actually, not only the largest variations in the global potential field (and subsequently also in the global geoidal geometry) but also the largest differences between the

<sup>\*</sup> School of Geodesy and Geomatics, The Key Laboratory of Geospace Environment and Geodesy, Wuhan University, 129 Luoyu Road, Wuhan, 430079, China. Fax: +86 27 6877 1695.

potential field at the topographic surface and on the geoid mainly occur at the long-to-medium wavelengths. To investigate these differences we present the numerical method of computing the gravitational field quantities on the geoid from the external gravitational field model. This method utilizes expressions derived in the spectral domain for the gravimetric forward modelling of topographic masses and the indirect gravimetric modelling of masses distributed inside the geoid. The spectral expressions are recapitulated in Section 2. We then apply this method to compute globally the disturbing potential on the geoid and compare the result with the disturbing potential at the topographic surface. The used input data and methodologies are briefly reviewed in Section 3. The results are presented and discussed in Section 4 and concluded in Section 5.

#### 2. Theory

The external gravitational field of the Earth can - for convenience - be described by means of the disturbing potential T which is obtained from the Earth's gravitational potential W after subtracting the normal gravitational potential U, i.e., T = W - U. Adopting the Earth's spherical approximation, the disturbing potential T is defined by the following spectral representation (e.g., [26]; Chap. 2.14)

$$T(r,\Omega) \cong \frac{\mathsf{GM}}{\mathsf{R}} \sum_{n=0}^{\overline{n}} \left(\frac{\mathsf{R}}{r}\right)^{n+1} \sum_{m=-n}^{n} T_{n,m} Y_{n,m}(\Omega), \tag{1}$$

where GM is the geocentric gravitational constant (i.e., the product of Newton's gravitational constant G and the total mass of the Earth M), R is the Earth's mean radius (which approximates the geocentric radii of the geoid),  $Y_{n,m}$  are the (fully-normalized) surface spherical functions of degree n and order m, and  $\overline{n}$  is the upper limit of the series expansion. The (fully-normalized) numerical coefficients  $T_{n,m}$  of the disturbing potential are obtained from the coefficients of the global gravitational model (GGM) after subtracting the spherical harmonic coefficients of the normal gravitational model, adopting typically the parameters of the Geodetic Reference System 1980 (GRS80, [27]. The 3-D position in Eq. (1) and thereafter is defined in the spherical coordinate system  $(r,\Omega)$  where r is the spherical radius, and  $\Omega = (\phi, \lambda)$  is the spherical direction with the spherical latitude  $\phi$  and longitude  $\lambda$ .

The coefficients  $T_{n,m}$  describe the disturbing potential at (or above) the topographic surface. In this case, the disturbing potential satisfies the Poisson equation:  $\Delta T=0$  (while disregarding the actual atmospheric density distribution). Inside the Earth's masses, however, the disturbing potential holds for the Laplace equation:  $\Delta T=-4\pi~G\rho$ ; where  $\rho$  is the mass density distribution function. For  $\rho\neq 0$ , the expression in Eq. (1) cannot thus directly be used to describe the disturbing potential.

To define the disturbing potential on the geoid, we decompose the Earth's gravitational field into the topographic and non-topographic parts. The topographic part represents the gravitational contribution of topographic masses, while the non-topographic part accounts for the gravitational contribution of masses distributed inside the geoid. Adopting this decomposition, the disturbing potential T at the topographic surface  $(r_t, \Omega)$  becomes

$$T(r_t, \Omega) = T^{NT}(r_t, \Omega) + V^T(r_t, \Omega), \tag{2}$$

where  $T^{NT}$  is the no-topography disturbing potential [28] and  $V^T$  is the topographic potential. By analogy with Eq. (2), the disturbing potential on the geoid  $(r_g, \Omega)$  is written in the following form

$$T(r_{\sigma}, \Omega) = T^{NT}(r_{\sigma}, \Omega) + V^{T}(r_{\sigma}, \Omega). \tag{3}$$

The positions of computation points at the topographic surface and on the geoid in Eqs. (2) and (3) are specified by the geocentric radii  $r_t$  and  $r_g$ , respectively. In the spherical approximation, these geocentric radii are defined as  $r_t \cong \mathbb{R} + H$  and  $r_g \cong \mathbb{R}$ , where H denotes the topographic height.

Let us now rearrange the expression in Eq. (2) into the following form

$$T^{NT}(r_t, \Omega) = T(r_t, \Omega) - V^T(r_t, \Omega). \tag{4}$$

We also formally rewrite the expression in Eq. (3) as follows

$$T(r_{g},\Omega) = T^{NT}(r_{g},\Omega) - T^{NT}(r_{t},\Omega) + T^{NT}(r_{t},\Omega) + V^{T}(r_{g},\Omega).$$
 (5)

The substitution from Eq. (4) to Eq. (5) then yields  $T(r_g,\Omega) = T(r_t,\Omega) + \left[V^T(r_g,\Omega) - V^T(r_t,\Omega)\right] + \left[T^{NT}(r_g,\Omega) - T^{NT}(r_t,\Omega)\right]. \tag{6}$ 

The expression in Eq. (6) relates the disturbing potential values on the geoid and at the topographic surface by means of the topographic potential difference  $V^T(r_g,\Omega)-V^T(r_t,\Omega)$  and the notopography disturbing potential difference  $T^{NT}(r_g,\Omega)-T^{NT}(r_t,\Omega)$ . Following the procedure proposed in Ref. [29]; we further treat the topographic potential individually for the gravitational contributions of the (constant) reference and (spatially-variable) anomalous topographic density distributions. Applying this formalism, the expression in Eq. (6) becomes

$$T(r_{g},\Omega) = T(r_{t},\Omega) + \left[V^{T,\rho^{T}}(r_{g},\Omega) - V^{T,\rho^{T}}(r_{t},\Omega)\right] + \left[V^{T,\delta\rho^{T}}(r_{g},\Omega) - V^{T,\delta\rho^{T}}(r_{t},\Omega)\right] + \left[T^{NT}(r_{g},\Omega) - T^{NT}(r_{t},\Omega)\right]$$

$$(7)$$

where  $V^{T,\rho T}$  and  $V^{T,\delta \rho T}$  are the topographic potentials of the reference and anomalous topographic density, respectively.

The disturbing potential at the topographic surface in Eq. (7) is computed for  $r=r_t$  in the spectral domain according to the expression in Eq. (1). The topographic density contribution (i.e., the topographic potential difference) in Eq. (7) comprises the contributions of the masses with reference density and those of anomalous topographic density. The topographic density contribution is evaluated from available digital terrain and density models based on applying the gravimetric forward modelling. The computation of the non-topographic contribution (i.e., the no-topography disturbing potential difference) in Eq. (7) requires an additional numerical step of subtracting the topographic potential from the disturbing potential at the topographic surface. Taking into consideration the decomposition of the topographic potential into the reference and anomalous density contributions in Eq. (4), this numerical step is defined as

$$T^{NT}(r_t, \Omega) = T(r_t, \Omega) - V^{T, \rho^T}(r_t, \Omega) - V^{T, \delta \rho^T}(r_t, \Omega).$$
 (8)

The spectral expressions for computing the topographic and non-topographic components are reviewed below.

## 2.1. Topographic potential difference (of reference density)

The topographic potential difference (of the reference density) in Eq. (7) could be computed by means of Newton's volumetric integral defined for the internal and external convergence domains. In this case, the expression for the external convergence domain is

## Download English Version:

# https://daneshyari.com/en/article/5780627

Download Persian Version:

https://daneshyari.com/article/5780627

<u>Daneshyari.com</u>